ELSEVIER

Electron transfer in the reactions of titanocene-bis(trimethylsilyl)acetylene complexes with 2,2'-bipyridine and 4,5-diazafluorene. The crystal structure of (4,5-diazafluorenyl)bis(pentamethylcyclopentadienyl)titanium(III)

Peter T. Witte [a,1], René Klein [a], Huub Kooijman [b], Anthony L. Spek [b,2], Miroslav Polášek [c], Vojtech Varga [c], Karel Mach [c,*]

[a] *University of Amsterdam, Department of Inorganic Chemistry, Nieuwe Achtergracht 166, 1018 WV Amsterdam, Netherlands*
[b] *Bijvoet Center for Biomolecular Research, Department of Crystal and Structural Chemistry, Utrecht University, Padualaan 8, 3584 CH Utrecht, Netherlands*
[c] *J. Heyrovský Institute of Physical Chemistry, Academy of Sciences of the Czech Republic, Dolejškova 3, 182 23 Prague 8, Czech Republic*

Abstract

The titanocene-bis(trimethylsilyl)acetylene complexes $Cp'_2Ti[\eta^2-C_2(SiMe_3)_2]$ ($Cp' = C_5H_5$, C_5HMe_4, and C_5Me_5) react with 2,2'-bi-pyridine (bpy) to give the corresponding $Cp'_2Ti(bpy)$ complexes **1–3**. EPR evidence of the electronic triplet state in **1–3** implies the transfer of one of the Ti d^2 electrons to the bpy ligand. An analogous electron transfer to 4,5-diazafluorene (dafH) affords (4,5-diazafluorenyl)titanocene (Ti^{III}) complexes $Cp'_2Ti(daf)$ ($Cp' = C_5H_5$ **(4)**, C_5HMe_4 **(5)**, and C_5Me_5 **(6)**) with a release of one hydrogen atom from the sp^3 carbon atom of the ligand. EPR spectra of **4–6** in toluene solutions are characterized by $g = 1.9798–1.9820$, coupling to ^{47}Ti and ^{49}Ti isotopes $a_{Ti} = 11.9–12.6$ G, and for **4** and **6** also by the coupling to two equivalent nitrogen atoms $a_N \approx 2.0$ G. Rhombic g-tensors with g_{av} in the range 1.981–1.982 were obtained in frozen toluene glass. The X-ray crystal structure of **6** (monoclinic, $P2_1/c$ (No. 14), $a = 11.7309(9)$ Å, $b = 14.7075(10)$ Å, $c = 14.7893(11)$ Å, $\beta = 94.68(6)°$, $V = 2543.1(4)$ Å^3, $Z = 4$) proved that both nitrogen atoms of an approximately planar 4,5-diazafluorenyl ligand coordinate to a pseudotetrahedrally coordinated titanium atom. The electronic absorption spectra of **4–6** in solution showed a well-resolved vibrational structure of the (daf)$^-$ anion with positions of all vibronic bands shifted to longer wavelength by ca. 20–30 nm, and a low intensity band probably of the d–d transition in the range 820–940 nm.

1. Introduction

The titanocene (Ti^{II})–2,2'-bipyridine complex [1,2] is of great interest because it generates a thermally populated triplet state whose structure is believed to differ from the ground singlet state by the mode of coordination of the bipyridine (bpy) ligand [3]. The compound was obtained either by reaction of bpy with $Cp_2Ti(CO)_2$ [1] or by reduction of Cp_2TiCl_2 with sodium sand in the

presence of bpy [2]. The latter method was also used for the preparation of $(C_5H_4Me)_2Ti(bpy)$ complex, whose magnetic properties in solution, however, differed only negligibly from those of $Cp_2Ti(bpy)$ [3]. Recently, we have preliminarily reported the formation of titanocene · bpy complexes $Cp'_2Ti(bpy)$ (for $Cp' = C_5H_5$, C_5HMe_4, and C_5Me_5) from Cp'_2Ti-bis(trimethylsilyl)acetylene complexes by heating with an equimolar amount of bpy [4]. The use of bipyridine ligands annealed in 3,3'-positions by methylene chains $(CH_2)_n$ of different length [5] can lead to a variety of complexes with different properties. The distortion of the pyridine planes from planarity induced by the methylene chain for $n = 2$ to 4 has been proven in a series of ruthenium complexes [6]. In

---
* Corresponding author.
[1] Present address: University of Groningen, Department of Inor-ganic Chemistry, Nijenborgh 16, 9747 AG Groningen, Netherlands.
[2] Address correspondence regarding crystallography to this author.

contrast, the monomethylene-annealed bpy ligand 4,5-diazafluorene (dafH) is planar and offers various modes of coordination, through the nitrogen atoms, aromatic rings, central cyclopentadiene ring or σ- or π-cyclopentadienyl moiety.

Here we report different modes of the redox reaction of $Cp_2'Ti[\eta^2-C_2(SiMe_3)_2]$ complexes with 2,2'-bipyridine and 4,5-diazafluorene, the spectroscopic properties of the products formed and the X-ray structure of the $(C_5Me_5)_2Ti(daf)$ complex.

2. Experimental details

2.1. General data and methods

Synthesis, purification and crystallization procedures and measurements of EPR and UV–vis spectra in solution were carried out in evacuated all-sealed glass devices equipped with magnetically breakable seals. A combined device equipped with a pair of quartz cuvettes (1 cm and 1 mm) and a quartz ESR tube was used for the UV–vis and ESR measurements. ESR spectra were recorded on an ERS-220 spectrometer (Centre for Production of Scientific Instruments, Academy of Sciences of GDR, Berlin, Germany) in the X-band. g-Values were determined using an Mn^{2+} ($M_1 = -1/2$ line) standard at $g = 1.9860$ and a proton magnetometer MJ-110 R (Radiopan, Poznan, Poland). Concentrations of the paramagnetic compounds were estimated from integrated first derivation spectra. A variable temperature unit STT-3 was used for the measurement in the range -150 to $+20°C$. UV–vis spectra were registered in the range 280–2000 nm on a Varian Cary 17D spectrometer using all-sealed quartz cuvettes (Hellma). Mass spectra were measured on a JEOL D-100 spectrometer at 70 eV (only peaks of intensity not below 5% and important peaks of lower intensity are reported). Samples in capillaries were opened and inserted into the direct inlet under argon. Infrared spectra were obtained on a UR-75 (Ziess, Jena, Germany). Hexane solutions were filled into KBr cuvettes under argon; regions 2800–3000 cm^{-1} and 1400–1500 cm^{-1} were not registered because of total absorption due to the solvent. GC analyses of volatile products from the reaction systems were performed on a CHROM 5 gas chromatograph (Laboratory Instruments, Prague, Czech Republic) using 10% SE-30 on a Chromaton N-AW-DMCS column. Analogous GC-MS analyses were also carried out on a Hewlett Packard gas chromatograph (5890 series II) equipped with a mass spectrometric detector (5971 A) and a capillary column SPB-1 (Supelco). The presence of hydrogen above the frozen reaction mixtures with dafH was detected using an MI 1302 mass spectrometer (USSR).
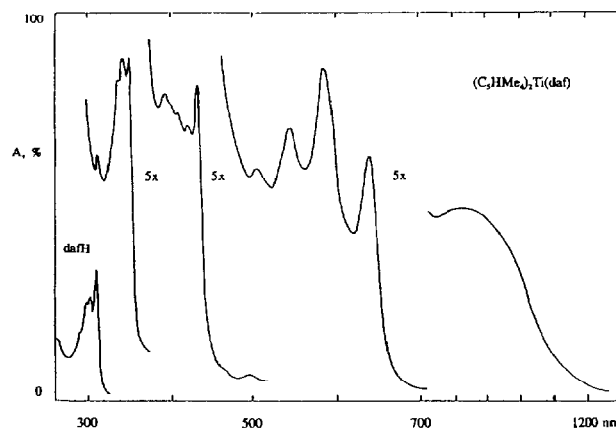

Fig. 1. Electronic absorption spectrum of $(C_5HMe_4)_2Ti(daf)$ (5) in hexane solution. The absorption spectrum of dafH is included near 300 nm.

2.2. Chemicals

The solvents hexane, toluene and tetrahydrofuran (THF) were purified by conventional methods, dried by refluxing over $LiAlH_4$, and stored as solutions of "dimeric titanocene" $(C_{10}H_8)[(C_5H_5)Ti(\mu-H)]_2$ [7]. Titanocene-bis(trimethylsilyl)acetylene complexes $(C_5H_5)_2Ti[\eta^2-C_2(SiMe_3)_2]$ [8], $(C_5HMe_4)_2Ti[\eta^2-C_2(SiMe_3)_2]$ [9], and $(C_5Me_5)_2Ti[\eta^2-C_2(SiMe_3)_2]$ [10] were prepared according to literature methods and were identical with those recently characterized in Ref. [9]. 2,2'-Bipyridine (bpy) was obtained from Fluka (puriss. p.a.) and was not further purified. 4,5-Diazafluorene (dafH) was obtained by the reduction of 4,5-diazafluoren-9-one with hydrazine hydrate [11]. The crude material was purified by liquid chromatography over the silica gel column using $CHCl_3$ as eluent. The crystallization from $CHCl_3$ gave colourless fine crystals, m.p. 171.5°C (lit. [12] m.p. 172°C). EI-MS, IR(KBr) and ^1H and ^{13}C NMR spectra did not indicate the presence of impurities. UV (hexane): 288, 296, 302, 309 nm (vibronic bands of the long wavelength electronic transition; see Fig. 1, bottom left).

2.3. Preparation of $(Cp')_2Ti(bpy)$ complexes 1–3

The solution of bpy in toluene (1.0 mmol in 4 ml) and the solution of $Cp_2'Ti[\eta^2-C_2(SiMe_3)_2]$ in hexane (0.25 M, 4 ml) were mixed together in an evacuated ampoule. The ampoule was sealed off and then heated to 60°C for 5 h to obtain 1, to 120°C for 2 h to obtain 2, and to 120°C for 6 h to obtain 3. A dark-green solution of 1 and brown solutions of 2 or 3 were evaporated in vacuum and the volatiles were collected for GC or GC-MS analyses. The dark residues were extracted with hot hexane and crystallized by cooling. The volatiles contained bis(trimethylsilyl)acetylene (BTMSA) in a

quantity roughly corresponding to the amount of $Cp'_2Ti[\eta^2\text{-}C_2(SiMe_3)_2]$ taken into the reaction.

$(C_5H_5)_2Ti(bpy)$ (1) was obtained as dark blue needles. Yield 0.22 g (65%). MS (110°C; m/e (%)): 334 $(M^+; 30.7)$, 269 $([M-C_5H_5]^+; 6.9)$, 190(5.6), 180(8.5), 179(18.4), 178 $([M-bpy]^+; 100)$, 177(12.0), 176(12.0), 167 $(M^{2+}; 5.3)$, 156(37.3), 155(18.7), 152(6.4), 134.5 $([M-C_5H_5]^{2+}; 18.1)$, 130(6.4), 129(10.1), 128(11.5), 113(17.3), 102(7.7), 95(10.0). EPR (toluene, 23°C): g = 1.995, ΔH = 80 G [Ti^{III} impurities were observed at g = 1.985 and g = 1.980, ΔH = 5 G]; (toluene, −130°C): g_x = 2.010, g_y = 1.990, g_z = 1.992, g_{av} = 1.997, D = 0.0415 cm^{-1}, E = 0.0025 cm^{-1}. UV–vis (toluene) (nm): 370 (s), 465 (m), 600 (w), 770 (w). IR (hexane) (cm^{-1}): 1290 (m), 1280 (sh), 1265 (s), 1147 (m), 1124 (w), 1030 (w), 1010 (m), 960 (s), 790 (vs), 695 (vs), 465 (s).

$(C_5HMe_4)_2Ti(bpy)$ (2) was obtained as black–blue cubes. Yield 0.35 g (80%). MS (140°C; m/e (%)): 446 $(M^+; 22.7)$, 325 $([M-C_5HMe_4]^+; 4.8)$, 323(9.3), 290 $([M-bpy]^+; 100)$, 244(8.3), 223 $(M^{2+}; 6.1)$, 167(7.4), 162.5 $([M-C_5HMe_4]^{2+}; 7.5)$, 156(11.0), 155(6.8), 102(5.0). EPR (toluene, 23°C): g = 1.998, ΔH = 62 G; (toluene, −196°C): g_x = 2.008, g_y = 1.985, g_z = 1.993, g_{av} = 1.995, D = 0.0405 cm^{-1}, E = 0.0029 cm^{-1}. UV–vis (toluene) (nm): 310 (sh), 385 (s), 490 (m), 520 (sh), 855 (w, broad). IR (toluene) (cm^{-1}): 1285 (s), 1275 (s), 1260 (vs), 1200 (m), 1140 (s), 1120 (m), 1085 (w), 1010 (s), 950 (vs), 650 (w), 610 (m), 435 (m).

$(C_5Me_5)_2Ti(bpy)$ (3) was obtained as dark brown needles. Yield 0.35 g (75%). MS (165°C; m/e (%)): 474 $(M^+; 15.1)$, 339 $([M-C_5Me_5]^+; 7.4)$, 338(6.5), 337(17.3), 335(7.9), 320(10.5), 319(28.6), 318 $([M-bpy]^+; 100)$, 317(19.6), 316(18.4), 260(7.0), 258(9.1), 237 $(M^{2+}; 5.0)$, 181(9.0), 178(6.0), 177(5.4), 169.5 $([M-C_5Me_5]^{2+}; 6.4)$, 156(19.6), 155(9.7), 128(5.7). EPR (toluene, 23°C): g = 1.997, ΔH = 56 G; (toluene, −196°C): g_x = 2.007, g_y = 1.986, g_z = 1.991, g_{av} = 1.995, D = 0.0395 cm^{-1}, E = 0.0026 cm^{-1}. UV–vis (toluene) (nm): 355 (sh), 390 (s), 490 (m), 520 (m), 870 (w, broad). IR (hexane) (cm^{-1}): 1540 (m), 1290 (s), 1280 (s), 1265 (vs), 1205 (m), 1140 (s), 1120 (m), 1090 (m), 1025 (w), 1010 (m), 955 (vs), 750 (s), 680 (m), 610 (w), 465 (w), 435 (w).

All the mass spectra contain ions of bpy m/e 156, 155, 130, 129, 128, 78 in the intensity ratio corresponding to free bpy. They can arise from the fragmentation of the complexes or from the ionisation of bpy liberated in thermal dissociation of the complexes on walls of the ionisation chamber.

2.4. Preparation of (Cp')₂Ti(daf) complexes 4–6

Freshly recrystallized dafH (0.168 g, 1 mmol) was dissolved in toluene (8 ml) and a solution of $Cp'_2Ti[\eta^2$

−$C_2(SiMe_3)_2]$ in hexane (0.25 M, 4 ml) was added. The reaction mixture was worked up after warming to 60°C for 2 h to obtain 4, 100°C for 1 h to obtain 5, and 100°C for 2 h to obtain 6. Red–brown solutions were obtained in all cases. These were cooled by liquid nitrogen and a volume above the frozen solution was investigated by MS for the presence of hydrogen. After warming, all volatiles were evaporated at 40°C in vacuo and were subject to GC and/or GC-MS analysis. Dark brown residues were extracted with hexane until the colouration of the extracted solution faded. The concentrated hexane solutions were cooled and the separated solids were recrystallized from hexane by a slow, continuous cooling. A dark brown amorphous solid was obtained for 4, whereas 5 and 6 afforded crops of black crystals. The solutions of 4 were pale greenish in incident light and pale purple in transmitted light. The solutions of 5 and 6 behaved similarly but their colours were more intense. The yields of crystalline solids obtained after the volume reduction to ca. 2 ml ranged from 60–80%. The volatiles from the reactions contained BTMSA as the only product from the initial $Cp'_2Ti[\eta^2 - C_2(SiMe_3)_2]$ complexes (cf. Ref. [9]).

$(C_5H_5)_2Ti(daf)$ (4). Yield 0.21 g (60%). MS (125°C; m/e (%)): 345 $(M^+; 43.8)$, 344(6.1), 280 $([M-C_5H_5]^+; 25.3)$, 179(18.4), 178 $([M-daf]^+; 100)$, 177(11.7), 176(11.7), 172.5 $(M^{2+}; 3.8)$, 168(21.5), 167(6.0), 140 $([M-C_5H_5]^{2+}; 11.4)$, 113(15.7), 107.5 $([M-C_{10}H_{10}]^{2+}; 3.6)$. EPR (hexane, 23°C): g = 1.9820, a_{Ti} = 12.5 G, a_N = 2.0 G at −56°C; (toluene, 23°C): g = 1.9819, a_{Ti} = 12.6 G; (toluene, −130°C): g_1 = 2.0007, g_2 = 1.9886, g_3 = 1.9572, g_{av} = 1.982. UV–vis (hexane) (nm): λ_1 (300 (sh), 307, 314 (sh), 321 (sh), 332, 340, 347), λ_2 (373, 390, 399, 408, 423, 435), λ_3 (515, 547, 572 (sh), 593, 623, 650), 820 (sh, broad) (λ_n = electronic transition showing the listed vibronic bands). IR (hexane) (cm^{-1}): 1602 (m), 1545 (m), 1520 (w), 1310 (sh), 1300 (s), 1200 (s), 1195 (sh), 1125 (w), 1110 (w), 1075 (w), 1005 (m), 840 (m), 795 (vs), 775 (vs), 685 (vs), 665 (m), 535 (w), 465 (s).

$(C_5HMe_4)_2Ti(daf)$ (5). Yield 0.36 g (80%). MS (140°C; m/e (%)): 457 $(M^+; 42.9)$, 456(6.0), 337(7.8), 336 $([M-C_5HMe_4]^+; 21.5)$, 335(5.9), 334(6.6), 319(5.0), 292(10.2), 291(25.3), 290 $([M-daf]^+; 100)$, 289(17.4), 288(17.7), 228.5 $(M^{2+}; 5.6)$, 215(5.0), 168.5 $([M-C_5HMe_4]^{2+}; 5.3)$, 168(10.4). EPR (hexane, 23°C): g = 1.9816, a_{Ti} = 11.9 G; (toluene, 23°C): g = 1.9819, a_{Ti} = 11.9 G; (toluene, −130°C): g_1 = 2.0007, g_2 = 1.9885, g_3 = 1.9583, g_{av} = 1.982. UV–vis (hexane) (nm): λ_1 (297, 304 (sh), 310, 334 (sh), 340, 349), λ_2 (385, 405 (sh), 418, 429), λ_3 (502, 538, 585, 638), 920 (very broad). IR (hexane) (cm^{-1}): 1602 (w), 1545 (m), 1520 (w), 1310 (sh), 1300 (s), 1195 (s), 1125 (w), 1110 (w), 1080 (w), 1020 (m), 840 (s), 780 (vs), 685 (s), 660 (m), 535 (w), 465 (m).

$(C_5Me_5)_2Ti(daf)$ (6). Yield 0.36 g (75%). MS (160°C;

m/e (%)): 485 (M$^+$; 30.0), 353(11.1), 352(9.5), 351(14.1), 350 ([M–C$_5$Me$_5$]$^+$; 35.0), 349(7.9), 348(9.4), 333(5.9), 320(11.2), 319(29.0), 318 ([M–daf]$^+$; 100), 317(17.3), 316(16.0), 242.5 (M^{2+}; 4.5), 215(4.7), 188(5.1), 168(9.6). EPR (hexane, 23°C): $g = 1.9798$, $a_{Ti} = 12.2$ G; (toluene, $-35°C$): $g = 1.9803$, $a_{Ti} = 12.4$ G, $a_N = 2.05$ G); (toluene, $-130°C$): $g_1 = 2.0000$, $g_2 = 1.9883$, $g_3 = 1.9536$, $g_{av} = 1.981$. UV–vis (hexane) (nm): λ_1 (310, 332 (sh), 340, 348 (sh)), λ_2 (385, 395 (sh), 415, 430), λ_3 (500, 540, 580, 635), 940 (very broad). IR (hexane) (cm^{-1}): 1605 (m), 1545 (w), 1520 (vw), 1310 (sh), 1300 (s), 1200 (s), 1080 (w), 1030 (w), 848 (s), 780 (s), 760 (vs), 695 (vs), 665 (vw), 535 (vw), 465 (s).

The MS ions m/e 168, 141, 140, 114, 113 attributable to dafH may arise either from the fragmentation of the complexes or from the ionisation of dafH liberated in the thermal dissociation with a proton transfer of the complexes on walls of the ionisation chamber. Vibronic bands were observed on each of the λ_1, λ_2 and λ_3 electronic transitions of 4–6 (for the spectrum of 5 see Fig. 1).

2.5. Preparation of [(daf)$^-$Li$^+$] and its electronic absorption spectrum

A freshly prepared solution of BuLi (1.6 mmol in 10 ml of THF) was poured onto purified dafH (15 mg) to give instantly a red solution. This solution remained stable for at least two months. Its electronic absorption spectrum exerted a pattern of vibronic bands which was very similar to that observed in 4–6. UV–vis (THF) (nm): λ_1 (305 (sh), 313 (sh), 320, 327, 335 (s)), λ_2 (353 (sh), 368, 383, 395, 407 (s)), λ_3 (450, 482, 513 (s), 553 602) nm (sh shoulder, s the strongest vibronic band among those belonging to a particular electronic transition denoted λ_n).

2.6. X-ray structure determination of 6

A dark opaque crystal suitable for X-ray structure determination was mounted on a Lindemann-glass capillary and transferred into the cold nitrogen stream of an Enraf-Nonius CAD4-T diffractometer on rotating anode. Accurate unit-cell parameters and an orientation

Table 1
Crystallographic data for 6

Crystal data	
Formula	$C_{31}H_{37}N_2Ti$
Molecular weight	485.53
Crystal system	monoclinic
Space group	$P2_1/c$ (No. 14)
a, b, c (Å)	11.7309(9), 14.7075(10), 14.7893(11)
β (°)	94.68(6)
V (Å^3)	2543.1(4)
Z	4
D_{calc} (g cm^{-3})	1.268
$F(000)$	1036
μ_{calc} (cm^{-1})	3.6
Crystal size (mm^3)	0.3 × 0.5 × 0.7
Data collection	
T (K)	150
$\theta_{min}, \theta_{max}$ (°)	1.38, 27.5
Radiation (Mo K α, graphite monochromator) (Å)	0.71073
Scan type	ω
$\Delta\omega$ (°)	0.65 + 0.35 tan θ
Horizontal, vertical aperture (mm)	2.35 + 1.15 tan θ, 4.00
Reference reflections	2 $\bar{1}$ 5, $\bar{4}$ $\bar{2}$ $\bar{1}$, 4 0 $\bar{2}$
Data set	$-15:15, -19:0, -19:15$
Total data	9718
Total unique data	5823 ($R_{int} = 0.035$)
Refinement	
No. refined parameters	418
Weighting scheme [a]	$w = 1/[\sigma^2(F^2) + (0.0437P)^2 + 1.50P]$
Final wR_2, R_1, S [b]	0.099, 0.043 [for 4338 $I > 2\sigma(I)$], 1.02
$(\Delta/\sigma)_{av}$, $(\Delta/\sigma)_{max}$ in final cycle	0.000, 0.002
Min., max. residual density (e Å^{-3})	-0.23, 0.30

[a] $P = [\max(F_o^2, 0) + 2F_c^2]/3$.

[b] $R_1 = \Sigma ||F_o| - |F_c||/\Sigma|F_o|$, $wR_2 = [\Sigma[w(F_o^2 - F_c^2)^2]/\Sigma[w(F_o^2)^2]]^{1/2}$.

matrix were determined by least-squares fitting of the setting angles of 25 well-centred reflections (SET4 [13]) in the range $11.44° < \theta < 13.93°$. Reduced-cell calculations did not indicate higher lattice symmetry [14]. Crystal data and details on data collection and refinement are given in Table 1. Data were corrected for Lorentz and polarization effects and for a linear decay of 1% of the three periodically measured reference reflections during 21 h of X-ray exposure time. Data were not corrected for absorption.

The structure was solved by automated Patterson methods and subsequent difference Fourier techniques (DIRDIF-92 [15]). Refinement on F^2 was carried out by full-matrix least-squares techniques (SHELXL-93 [16]; no observance criterion was applied during refinement). All hydrogen atoms were located on a difference Fourier map and their positional parameters were subsequently included in the refinement. Non-hydrogen atoms were refined with anisotropic thermal parameters. The hydro-

gen atoms were refined with a fixed isotropic thermal parameter related to the value of the equivalent isotropic displacement parameter of their carrier atoms by a factor of 1.5 for the methyl hydrogen atoms and a factor of 1.2 for the aromatic hydrogen atoms.

Neutral atom scattering factors and anomalous dispersion corrections were taken from the *International Tables for Crystallography* [17]. Geometrical calculations and illustrations were performed with PLATON [18] and PLUTON [19]; all calculations were performed on a DEC station 5000.

3. Results and discussion

3.1. The formation of $(Cp')_2Ti(bpy)$ $(Cp' = C_5H_5$ (1), C_5HMe_4 (2), and C_5Me_5 (3)) complexes

The $Cp'_2Ti[\eta^2-C_2(SiMe_3)_2]$ complexes react with one equivalent of bpy in a toluene/hexane mixture to give

Table 2

Final coordinates and equivalent isotropic thermal parameters of the non-hydrogen atoms of **6**

Atom	x	y	z	U_{eq} (Å^2) [a]
Ti(1)	0.25294(3)	0.04466(2)	0.22478(2)	0.0172(1)
N(1)	0.20717(14)	−0.01430(12)	0.35762(11)	0.0232(5)
N(2)	0.30552(13)	−0.10039(11)	0.20638(11)	0.0215(5)
C(1)	0.2330(2)	−0.10351(14)	0.35457(13)	0.0233(6)
C(2)	0.1610(2)	0.0130(2)	0.43245(14)	0.0294(6)
C(3)	0.1433(2)	−0.0480(2)	0.50406(15)	0.0388(9)
C(4)	0.1656(2)	−0.1396(2)	0.4989(2)	0.0369(8)
C(5)	0.2151(2)	−0.1720(2)	0.42108(14)	0.0296(7)
C(6)	0.2515(2)	−0.2560(2)	0.3871(2)	0.0351(7)
C(7)	0.2908(2)	−0.24041(14)	0.30008(14)	0.0271(6)
C(8)	0.3333(2)	−0.2918(2)	0.2303(2)	0.0346(7)
C(9)	0.3640(2)	−0.2464(2)	0.1543(2)	0.0319(7)
C(10)	0.3490(2)	−0.15226(15)	0.14320(14)	0.0250(6)
C(11)	0.2790(2)	−0.14509(14)	0.28154(13)	0.0220(6)
C(12)	0.4529(2)	0.04359(14)	0.28243(12)	0.0221(6)
C(13)	0.3992(2)	0.10617(14)	0.33744(13)	0.0224(6)
C(14)	0.3558(2)	0.17875(13)	0.28293(13)	0.0229(6)
C(15)	0.3868(2)	0.16265(13)	0.19279(13)	0.0218(6)
C(16)	0.4446(2)	0.07845(14)	0.19221(13)	0.0223(6)
C(17)	0.5206(2)	−0.0376(2)	0.3165(2)	0.0313(7)
C(18)	0.4035(2)	0.1013(2)	0.43910(14)	0.0325(7)
C(19)	0.3058(2)	0.2642(2)	0.3184(2)	0.0340(8)
C(20)	0.3901(2)	0.2308(2)	0.1175(2)	0.0310(7)
C(21)	0.5059(2)	0.0431(2)	0.11446(15)	0.0308(7)
C(22)	0.0481(2)	0.00730(14)	0.19826(13)	0.0235(6)
C(23)	0.0619(2)	0.10310(14)	0.20480(13)	0.0235(6)
C(24)	0.1199(2)	0.13212(14)	0.12898(13)	0.0240(6)
C(25)	0.1474(2)	0.05319(14)	0.07881(13)	0.0238(6)
C(26)	0.1001(2)	−0.02278(14)	0.12064(13)	0.0236(6)
C(27)	−0.0218(2)	−0.0516(2)	0.2550(2)	0.0316(7)
C(28)	0.0066(2)	0.1646(2)	0.2692(2)	0.0329(7)
C(29)	0.1189(2)	0.2287(2)	0.0970(2)	0.0329(7)
C(30)	0.2011(2)	0.0500(2)	−0.01007(14)	0.0317(7)
C(31)	0.0916(2)	−0.1176(2)	0.0836(2)	0.0318(7)

[a] U_{eq} is defined as one third of the trace of the orthogonalized U_{ij} tensor.

Table 3
EPR spectra of $Cp'_2Ti(bpy)$ (1–3) and $Cp'_2Ti(daf)$ (4–6) complexes in toluene solution and frozen glass

	g_{iso}	ΔH (G)	a_{Ti} (G)	g_x	g_y	g_z	g_{av}	D (cm^{-1})	E (cm^{-1})
1	1.995	80 [a]	—	2.010	1.990	1.992	1.997	0.0415	0.0025
	1.99		—	2.013	1.990	1.993	—	0.0412	0.0025 [b]
2	1.998	62	—	2.008	1.985	1.993	1.995	0.0405	0.0029
3	1.997	56	—	2.007	1.986	1.991	1.995	0.0395	0.0026
4	1.9819	6.8 [c]	12.6	2.0007	1.9886	1.9572	1.982	—	—
5	1.9818	6.7	11.9	2.0007	1.9885	1.9583	1.982	—	—
6	1.9803	6.9 [c]	12.4	2.0000	1.9883	1.9536	1.981	—	—

[a] The Ti^{III} impurities were observed at $g = 1.985$, $\Delta H = 5.0$ G and at $g = 1.980$, $\Delta H = 5$ G.
[b] Data from Ref. [3].
[c] A quintuplet splitting due to $a_N = 2.0$ G was optimally resolved at $-6°C$.

$Cp'_2Ti(bpy)$ ($Cp' = C_5H_5$ (1), C_5HMe_4 (2), and C_5Me_5 (3)) complexes in high yields [Eq. (1)]:

$$Cp'_2Ti[\eta^2-C_2(SiMe_3)_2] + bpy$$

$$\rightarrow (Cp')_2Ti(bpy) + C_2(SiMe_3)_2 \qquad (1)$$
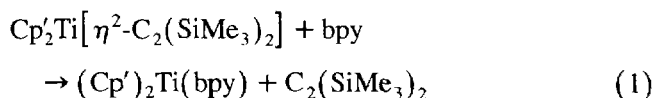
The reaction was accelerated by heating to 60°C for 1 and 120°C for 2 and 3, as the reactivity of the acetylene complexes decreases from the C_5H_5 to the C_5Me_5 complex. Compounds 1–3 were identified by their EI-MS spectra, showing molecular ions and doubly ionized molecular ions. The major fragmentation pathway of

$M^{+\cdot}$ ions involves the loss bpy, and the minor one the elimination of Cp'. The M^{2+} ions lose the Cp' ligands. Compound 1 is, according to its EPR spectrum and temperature-dependent behaviour, identical to $(C_5H_5)_2Ti(bpy)$ whose EPR spectra and structure have been thoroughly studied by Stucky and coworkers [3]. The EPR spectrum of the toluene solution showed a broad signal at $g = 1.995$, assigned to 1, and sharp signals at $g = 1.985$ and $g = 1.980$ of Ti^{III} impurities. The signal at $g = 1.995$ further broadened with lowering of the temperature and at $-130°C$, in frozen glass, a very weak EPR spectrum typical of the electronic triplet
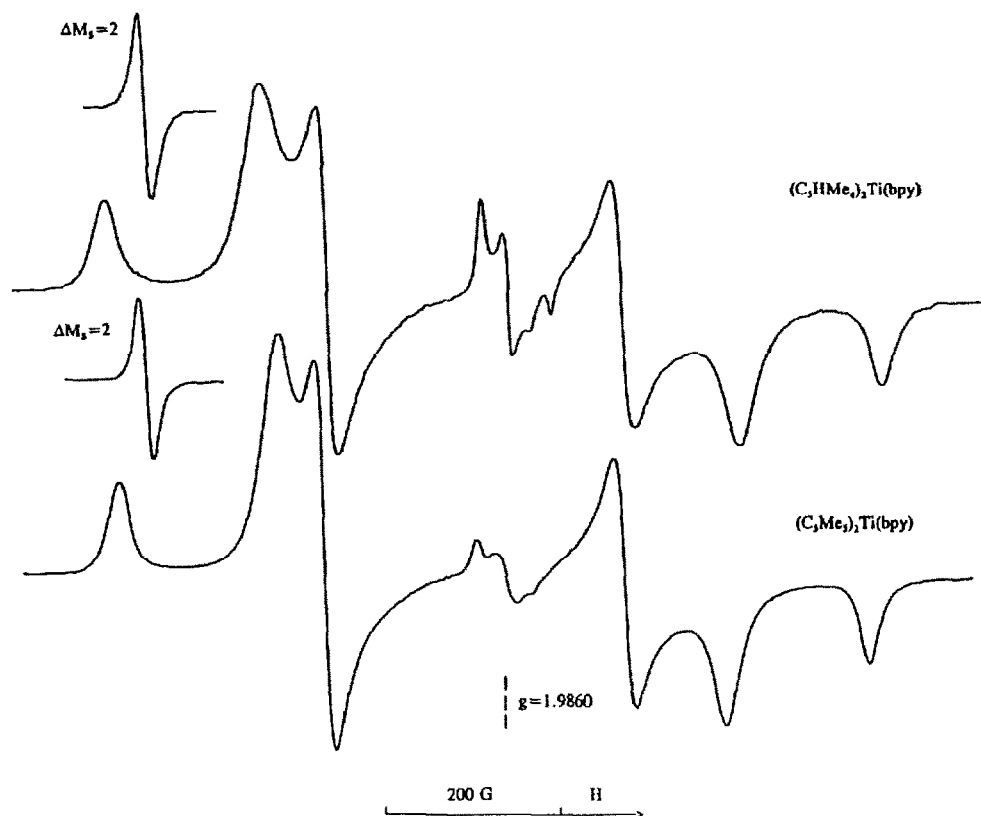

Fig. 2. EPR spectra of $(C_5HMe_4)_2Ti(bpy)$ (2) and $(C_5Me_5)_2Ti(bpy)$ (3) in frozen toluene glass at $-196°C$. The $\Delta M_s = 2$ transition was measured with the same amplification as the $\Delta M_s = 1$ spectrum and is shown at arbitrary magnetic field.

state of rhombic symmetry was obtained. Its g-tensor and zero field parameters D and E (Table 3) are very similar to those reported [3]. It was also reported that the intensity of this spectrum decreased with lowering of the temperature of the glassy sample, implying that the triplet state is thermally populated from the ground singlet state. Accordingly, the EPR spectrum of the triplet state nearly disappeared at $-196°C$ [3]. Our EPR results are in qualitative agreement with those described above (Table 3). The decrease in intensity of the $\Delta M_s = 2$ transition with lowering temperature in the range -120 to $-150°C$ was estimated to be not higher than 10%. In contrast, the EPR spectra of Ti^{III} impurities grew in intensity with decreasing temperature, and in the toluene glass gave a rhombic g-tensor (Table 3) with g_x and g_y components typical for the $Cp_2'Ti^{III}$ fragment [20].

Compounds 2 and 3 afforded broad signals in toluene solution with only negligible signals of Ti^{III} impurities. In toluene glass at $-130°C$ the triplet state spectra of very similar parameters to those of 1 were obtained (Fig. 2, Table 3). The intensity of the triplet state spectrum of 2 was ca. ten times higher than that of 1, and the intensity of the $\Delta M_s = 2$ transition decreased by only 6% between $-120°C$ and $-150°C$. Compound 3 afforded the triplet state spectrum with a significantly lower zero field splitting D than 1 and 2, and its intensity was about six times higher than that of 2. In contrast to both 1 and 2, the intensity of the $\Delta M_s = 2$ transition grew, on going from $-120°C$ to $-150°C$, by about 30%. This proves that the triplet state in 3 is, in contrast to 1 and 2, more stable in this temperature range than the singlet state. Quantitative measurements at lower temperatures are required to establish the nature of the ground state.

The electronic structure of 1 was discussed in terms of a titanocene Ti^{III} center bound to a bipyridine radical anion arising from an electron transfer of one of the Ti d^2 electrons to the bpy ligand [3]. The molecular structure of 1 was determined by X-ray single crystal diffraction analysis with a low accuracy by Stucky and coworkers [3]. The molecule was monomeric with a Ti–N distance of 2.14(2) Å and an angle between the plane of the bpy ligand and the N–Ti–N plane of 25(1)°. The results of MO calculations suggest that the singlet state geometry is the bent one, whereas the triplet state geometry should have the N–Ti–N plane coplanar with the plane of the bpy ligand [3]. The distance R between the Ti d^1 electron and the bpy radical anion, which form the triplet state, was calculated from the value of the zero field splitting parameter D to be roughly 3.5 Å, using a simplified relationship $R = (g^2\beta^2/D_d)^{1/3}$ ($D = D_d + D_e$), where D is assumed to arise solely from the dipolar interaction D_d [3] and the pseudo-dipolar component D_e equals zero. This assumption provides a good approximation for most of

the Ti^{III}–Ti^{III} dimers forming a triplet state [21–24]. We have calculated R values for 2 and 3 using Eq. (2) [21], with rhombic g-tensor values from Table 3 and assuming $D = D_d$:

$$D_d = -\beta^2/3R^3\left[2g_z^2 + \left(g_x^2 + g_y^2\right)/2\right] \quad (2)$$

The obtained values $R(2) = 3.48$ Å and $R(3) = 3.52$ Å virtually coincide with $R(1)$, however, they are all considerably larger than the crystallographic Ti–N distance of 2.14 Å for 1 [3]. This discrepancy can be accounted for by the delocalization of the transferred electron over the two nitrogen atoms of bpy and by a non-zero contribution of D_e. In contrast, the difference between $R(2)$ and $R(3)$ close to 0.04 Å should be more realistic. Our attempts to throw more light onto the geometry of either electronic state by determining the X-ray crystal structures of complexes 1–3 are under way.

3.2. The formation of $(Cp')_2Ti(daf)$ $(Cp' = C_5H_5$ (4), C_5HMe_4 (5), and C_5Me_5 (6) complexes

The reaction of $Cp_2'Ti[\eta^2-C_2(SiMe_3)_2]$ complexes with 4,5-diazafluorene (dafH) differed from that with bpy by the subsequent decomposition of a transient radical anion of dafH, yielding the daf anion and hydrogen. Thus $(Cp')_2Ti(daf)$ complexes 4 $(Cp' = C_5H_5)$, 5 $(Cp' = C_5HMe_4)$, and 6 $(Cp' = C_5Me_5)$ were obtained according to redox reaction (3):

$$Cp_2'Ti^{II}\left[\eta^2-C_2(SiMe_3)_2\right] + dafH$$

$$\rightarrow (Cp')_2Ti^{III}(daf) + C_2(SiMe_3)_2 + H^\cdot \quad (3)$$
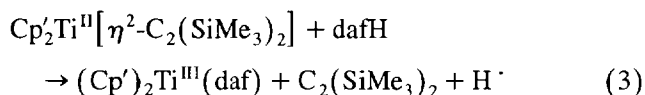
The EI-MS spectra of 4–6 showed molecular ions $[Cp_2'Ti(daf)]^{+\cdot}$ and fragmentation patterns characterized by ions $[M-Cp']^+$ and the most abundant $[M-daf]^+$. The doubly ionized molecular ions were also observed, and they fragmented exclusively with the elimination of the Cp' ligands. The GC-MS analysis of volatile reaction products proved that the liberated BTMSA is not accompanied by bis(trimethylsilyl)-ethenes or bis(trimethylsilyl)ethane. Gaseous hydrogen was detected by MS above the frozen reaction mixture, however, its quantity was not determined.

The presence of Ti^{III} in 4–6 was unequivocally proven by the EPR spectra of the toluene solutions and frozen glasses, showing typical features of titanocene(III) derivatives (Table 3) [20]. The EPR spectra of all the compounds in solution exerted a sharp signal at $g = 1.980–1.982$ ($\Delta H \leq 7.0$ G), accompanied by approximately 20 times weaker satellite peaks due to coupling to ^{49}Ti ($I_N = 7/2$) and ^{47}Ti ($I_N = 5/2$) isotopes $a_{Ti} = 11.9–12.5$ G. This coupling is large compared with that of $[Cp_2Tibpy]^+[PF_6]^-$ ($g = 1.98$), where a_{Ti} was only 8 G [3]. This indicates a lower delocalization of the unpaired d^1 electron at the daf anion com-
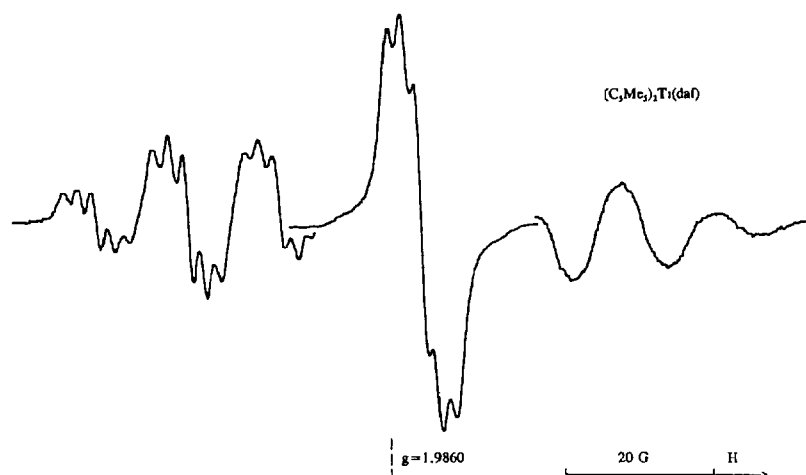
Fig. 3. EPR spectrum of $(C_5Me_5)_2Ti(daf)$ (6) in hexane solution measured at $-6°C$. The wing spectra due to the coupling to ^{49}Ti and ^{47}Ti isotopes are amplified twenty times.

pared with the bpy ligand in the above ionic salt. The EPR spectrum of 6 at $-6°C$ further showed a well-resolved quintuplet hyperfine splitting apparently arising from the coupling to two equivalent nitrogen nuclei ($a_N = 2$ G) (Fig. 3). The EPR spectra of frozen toluene glasses gave g-tensors typical of tetrahedrally coordinated $Cp'_2Ti(III)$ complexes, e.g. $Cp_2TiCl(THF)$ [20]. The reason for the coupling to nitrogen nuclei follows from the X-ray structure of 6 (vide infra) which confirms the presence of the daf anion and reveals its bonding to Ti^{III} by the coordination of nitrogen atoms.

The electronic absorption spectra of the complexes in solution show a vibronic structure on all absorption bands except the broad band at the longest wavelength (Fig. 1). A very similar vibronic pattern was observed in the absorption spectrum of $[(daf)^- Li^+]$, except that all the bands were shifted by about 20–30 nm to shorter wavelength. This implies that the vibrational modes of the daf anion, which are involved in the electronic transitions, are not influenced by the coordination of the daf ligand to the Ti atom. The presence of Ti^{III} in the molecule is demonstrated, besides the above mentioned shifts of the daf$^-$ spectrum to longer wavelength, by the presence of a broad band of low intensity in the range 820 (for 4) to 940 nm (for 6). A full analysis of the electronic and vibrational transitions in complexes 4–6 and in the daf anion is behind the scope of this work. The theoretical treatment of the problem will, however, be facilitated by the knowledge of the molecular structure of 6.

Table 4
Selected bond distances (Å) and bond angles (°) for 6

| Bond distances			
Ti(1)–N(1)	2.2521(17)	Ti(1)–N(2)	2.2434(16)
N(1)–C(1)	1.348(3)	N(2)–C(11)	1.349(3)
N(1)–C(2)	1.333(3)	N(2)–C(10)	1.339(3)
C(2)–C(3)	1.416(4)	C(9)–C(10)	1.404(4)
C(3)–C(4)	1.376(4)	C(8)–C(9)	1.380(4)
C(4)–C(5)	1.413(4)	C(7)–C(8)	1.403(4)
C(5)–C(6)	1.413(4)	C(6)–C(7)	1.421(4)
C(1)–C(5)	1.435(3)	C(7)–C(11)	1.433(3)
C(1)–C(11)	1.388(3)	C–C(Me)$_{av}$	1.499(4)
C–C(CE(1))$_{av}$	1.417(3)	C–C(CE(2))$_{av}$	1.420(3)
Ti(1)–CE(1)	2.105(1)	Ti(1)–CE(2)	2.105(1)
Bond angles			
N(1)–Ti(1)–N(2)	80.05(9)	CE(1)–Ti(1)–CE(2)	142.72(7)
Ti(1)–N(1)–C(1)	105.98(14)	Ti(1)–N(2)–C(11)	106.21(14)
Ti(1)–N(1)–C(2)	138.60(18)	Ti(1)–N(2)–C(10)	138.64(15)
N(1)–C(1)–C(11)	123.88(19)	N(2)–C(11)–C(1)	123.8(2)
C(1)–C(11)–C(7)	108.65(19)	C(11)–C(1)–C(5)	108.2(2)
C(1)–C(5)–C(6)	107.7(2)	C(11)–C(7)–C(6)	107.3(2)
C(5)–C(6)–C(7)	108.1(2)		
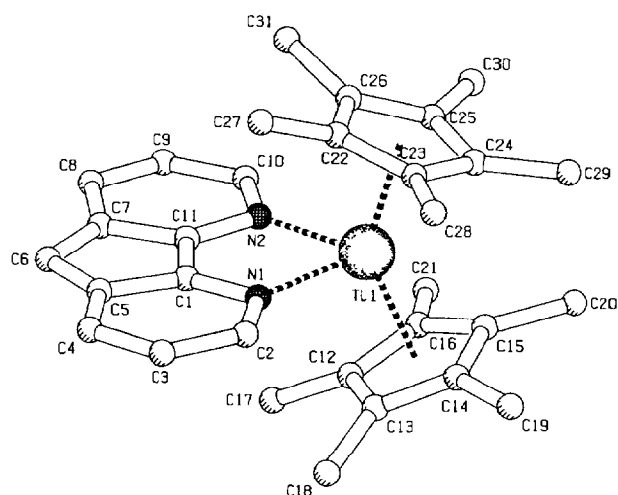
Fig. 4. PLUTON drawing [19] of the molecular structure and adopted atom numbering scheme of $(C_5Me_5)_2Ti(daf)$ (6).

3.3. Crystal structure of 6

A PLUTON drawing of the molecular structure of 6 and the atom numbering scheme are shown in Fig. 4. Selected bond lengths and angles are listed in Table 4. The absence of molecular symmetry is seen in partly staggered permethylcyclopentadienyl rings, as well as in different Ti–N(1) and Ti–N(2) bond lengths and a distorted daf ligand. The daf anion is approximately planar and the dihedral angle between the least-squares plane defined by N(1), N(2), C(1) and C(11) and the plane of the angle N(1)–Ti–N(2) is 1.76(12)°. The plane of the CE(1)–Ti–CE(2) angle is virtually perpendicular to the N(1), Ti, N(2) plane (89.78(9)°). The CE(1), Ti, CE(2) plane only roughly bisects the daf ligand, as the C(6) atom is 0.071(3) Å away from the plane and the carbon atoms of the C(1)–C(11) bond are 0.637(2) and 0.731(2) Å respectively away from the plane on opposite sides. The daf ligand has all N–C bonds shorter than 1.35 Å. Among the C–C bonds only C(3)–C(4) and C(8)–C(9) are close to 1.38 Å, and C(1)–C(11) is close to 1.39 Å. All the other C–C bonds fall into the interval 1.40–1.43 Å. The geometry of the central cyclopentadienyl ring of daf is fully consistent with the presence of only one hydrogen atom bonded to C(6). The hydrogen was detected on the difference Fourier map and was included in the refinement. The bond lengths Ti–N (av. 2.25 Å) are 0.32 Å longer than the analogous bonds in a 1,4-diaza-1,3-butadiene complex $(C_5H_5)Ti(DAD)Cl$ (DAD = 1,4-bis(4-methoxyphenyl)-2,3-dimethyl-1,4-diazabutadiene) (7) [25]. Correspondingly, the N(1)–Ti–(N2) angle in 6 is 8° smaller than that in 7. The bonds from nitrogen atoms to adjacent carbon atoms in 6 are ca. 0.05 Å shorter than in 7, however the C(1)–C(11) bond is of equal length with the analogous bond in 7. The steric strain in the permethyltitanocene moiety arising from the region

where the ligands approach each other is relieved partly by a staggered conformation, and partly by bending of Me groups from the ring plane farther away from the titanium atom. The CE(1)–Ti–CE(2) angle, 142.72(7)°, is closer to the value of 143.6° for $(C_5Me_5)_2TiCl$ [26] than to that of 137.4° for $(C_5Me_5)_2TiCl_2$ [27]. The closest contacts between the Me carbon atoms of the Cp* ligands and daf atoms appear between C(27)–N(1) (3.026(3) Å) and C(17)–N(2) (3.033(3) Å). Relatively long Ti–N bonds in 6 (compared, for example, with 7) indicate a relatively weak coordination bonding of the daf anion system to the titanium atom. This is in agreement with the assignment of the electronic absorption spectrum of 6 to a slightly disturbed daf anion whose molecular vibrations are little influenced by the Ti–N coordination.

4. Supplementary material available

Listings of atomic coordinates, bond lengths and angles and thermal parameters have been deposited at the Cambridge Crystallographic Data Centre. These, together with lists of observed and calculated structure factors and further details of the structure determination, are available from the authors (A.L.S.)

References

[1] E.O. Fischer and R. Aumann, J. Organomet. Chem., 9 (1967) P15.
[2] F. Calderazzo, J.J. Salzmann and P. Mosmann, Inorg. Chim. Acta, 1 (1967) 65.
[3] A.M. McPherson, B.F. Fieselmann, D.L. Lichtenberger, G.L. McPherson and G.D. Stucky, J. Am. Chem. Soc., 101 (1979) 3425.
[4] P.T. Witte, V. Varga and K. Mach, II Regional Seminar of Ph.D Students in Organometallic Chemistry, Prague, December 1–3, 1994, Abstr. p. 52.
[5] R.P. Thummel, F. Lefoulon and R. Mahadevan, J. Org. Chem., 50 (1985) 3824–3828.
[6] R.P. Thummel, F. Lefoulon and J.D. Korp, Inorg. Chem., 26 (1987) 2370.
[7] H. Antropiusová, A. Dosedlová, V. Hanuš and K. Mach, Transit. Met. Chem., 6 (1981) 90.
[8] V.V. Burlakov, U. Rosenthal, P.V. Petrovskii, V.B. Shur and M.E. Vol'pin, Metalloorg. Khim., 1 (1988) 953.

[9] V. Varga, K. Mach, M. Poláček, P. Sedmera, J. Hiller, U. Thewalt and S.I. Troyanov, J. Organomet. Chem., 506 (1996) 241.

[10] V.V. Burlakov, U. Rosenthal, R. Beckhaus, S.V. Polyakov, Yu.T. Struchkov, G. Oehme, V.B. Shur and M.E. Vol'pin, Metalloorg. Khim., 3 (1990) 476.

[11] K. Kloc, J. Mlochowski and Z. Szulc, J. Prakt. Chem., 319 (1977) 959.

[12] K. Kloc, J. Mlochowski and Z. Szulc, Heterocycles, 9 (1978) 849.

[13] J.L. de Boer and A.J.M. Duisenberg, Acta Crystallogr., A40 (1984) C410.

[14] A.L. Spek, J. Appl. Crystallogr., 21 (1988) 578.

[15] P.T. Beurskens, G. Admiraal, G. Beurskens, W.P. Bosman, S. García-Granda, R.O. Gould, J.M.M. Smits and C. Smykalla, The DIRDIF program system, Tech. Rep. of the Crystallography Laboratory, University of Nijmegen, Netherlands, 1992.

[16] G.M. Sheldrick, SHELXL-93, Program for crystal structure refinement, University of Göttingen, Germany, 1993.

[17] A.J.C. Wilson (ed.), International Tables for Crystallography, Vol. C, Kluwer Academic, Dordrecht, 1992.

[18] A.L. Spek, Acta Crystallogr., A46 (1990) C34.

[19] A.L. Spek, PLUTON, Molecular graphics program, Utrecht University, Netherlands, 1995.

[20] K. Mach and J.B. Raynor, J. Chem. Soc., Dalton Trans., (1992) 683.

[21] E. Samuel, J.F. Harrod, D. Gourier, Y. Dromzee, F. Robert and Y. Jeannin, Inorg. Chem., 31 (1992) 3252.

[22] D. Gourier, D. Vivien and E. Samuel, J. Am. Chem. Soc., 107 (1985) 7418.

[23] R. Gyepes, K. Mach, I. Císařová, J. Loub, J. Hiller and P. Šindelář, J. Organomet. Chem., 497 (1995) 33.

[24] R. Gyepes, J. Hiller, U. Thewalt, M. Poláček, P. Šindelář and K. Mach, J. Organomet. Chem., 516 (1996) 177.

[25] J. Scholz, A. Dietrich, H. Schumann and K.-H. Thiele, Chem. Ber., 124 (1991) 1035.

[26] J.W. Pattiasina, H.J. Heeres, F. van Bolhuis, A. Meetsma, J.H. Teuben and A.L. Spek, Organometallics, 6 (1987) 1004.

[27] T.C. McKenzie, R.D. Sanner and J.E. Bercaw, J. Organomet. Chem., 102 (1975) 457.